ARTICLES

Theoretical Investigation of the Electronically Excited States of Chlorine Hydrate

Daniel P. Schofield and Kenneth D. Jordan*

Department of Chemistry and Center for Molecular and Materials Simulations, University of Pittsburgh, Pittsburgh, Pennsylvania 15260

Received: April 20, 2007

As a step toward a first principles characterization of the optical properties of chlorine hydrate, we have calculated the electronic absorption spectrum of a chlorine molecule trapped in dodecahedral $(H_2O)_{20}$ and hexakaidodecahedral $(H_2O)_{24}$ cages. For comparison, spectra were also calculated for an isolated Cl_2 molecule as well as for selected $Cl_2(H_2O)_n$, $n \leq 8$, clusters cut out of the $Cl_2(H_2O)_{20}$ cluster, allowing us to follow the evolution of the low-lying excited states with increasing number of surrounding water molecules. Although encapsulation of a chlorine molecule within the water cages has relatively little effect on its low-lying valence transitions, it does result in a large number of solvent-to-solute charge-transfer transitions at energies starting near 48 000 cm^{-1}.

Introduction

Gas hydrates are solid nonstoichiometric materials consisting of inert gas atoms or small molecules encapsulated in rigid water cages.[1] The interaction between the guest species and the water lattice stabilizes the otherwise unstable water network. Much of the recent interest in hydrates has been centered on methane hydrate, which is the major reservoir for methane on earth.[1,2] Historically, the first hydrate discovered was that of chlorine, which was prepared by Humphry Davy in 1811.[3] X-ray diffraction measurements have shown that chlorine, like methane, forms a type I hydrate,[4] the periodic lattice of which contains two types of water cages. The smaller cages consist of $(H_2O)_{20}$ dodecahedra with 12 pentagonal faces (designated 5^{12}), and the larger cages consist of $(H_2O)_{24}$ hexakaidodecahedra with 12 pentagonal and 2 hexagonal faces (designated $6^2\,5^{12}$).

In spite of the fact that chlorine hydrate has been known for nearly two centuries, its UV−vis electronic absorption spectrum has not been reported in the literature. The paucity of experimental data on the electronically excited states of chlorine and other halogen hydrates may be due to the extremely high optical densities of the crystals.[5] In fact, it is only over the past year that the UV−vis spectrum has been obtained for bromine hydrate.[5] Interestingly, the optical spectrum of bromine hydrate displays intense, low-lying charge-transfer bands.

As an initial effort in the use of theoretical methods to elucidate the electronically excited states of halogen hydrates, we consider here a Cl_2 molecule encapsulated in $(H_2O)_{20}$ dodecahdral and $(H_2O)_{24}$ hexakaidodecahedral cages.[6] Experimentally, it has been found that essentially all the $6^2\,5^{12}$ cages but only about 30% of the 5^{12} cages of chlorine hydrate are occupied with Cl_2 molecules.[7,8] The low occupation of the 5^{12} cages is due to steric interactions.

In the present study the resolution of the identity approximate coupled-cluster singles-and-doubles (RICC2) method[9−11] is used to characterize the electronically excited states of the isolated Cl_2 molecule, the $Cl_2(H_2O)_{20}$ and $Cl_2(H_2O)_{24}$ clusters, as well as $Cl_2(H_2O)_n$, $n \leq 8$, clusters cut out from the $Cl_2(H_2O)_{20}$ cluster, thereby allowing us to follow the evolution of the excited states with increasing numbers of water molecules.

Computational Details

Before we turn to the electronic excitation spectra of the $Cl_2(H_2O)_{20}$ and $Cl_2(H_2O)_{24}$ systems, it is important to establish that the theoretical methods used properly describe the low-lying excited states of the isolated Cl_2 molecule. To this end, we have calculated the excitation energies of the low-lying excited states of Cl_2 using both the CC2[12] and CC3[13,14] methods. These calculations were performed at the experimental bond length[15] and employed the aug-cc-pVDZ,[16] aug-cc-pVTZ,[16] and aug-cc-pVTZ(+) basis sets, with the latter being formed by augmenting the aug-cc-pVTZ basis set with s-, p-, and d-function Rydberg Gaussian-type functions with exponents of 0.025, 0.02, and 0.015,[17] respectively, on each chlorine atom. The CC3 method includes higher order correlation effects absent in the CC2 method. These calculations provide a calibration of the CC2 and RICC2 methods as well as a check on the suitability of the aug-cc-pVDZ basis set for describing the low-lying excited states of Cl_2. As we will see below, the changes in going from the CC2 to CC3 method are quite small. Moreover, for the valence states, even the aug-cc-pVDZ basis set proves to be adequate, justifying the use of the RICC2 method and the aug-cc-pVDZ basis set for the $Cl_2(H_2O)_{20}$ and $Cl_2(H_2O)_{24}$ species.

There are 30 026 $(H_2O)_{20}$ "dodecahedral" structures that differ in the arrangement of the H bonds.[18,19] In a clathrate crystal, many of these arrangements will be sampled. In the present work, we employ a $(H_2O)_{20}$ dodecahedron that possesses inversion symmetry (C_i point group), to reduce the cost of the calculations. The chlorine molecule was located at the center

* To whom correspondence should be addressed. E-mail: jordan@imap.pitt.edu.

10.1021/jp073068a CCC: $37.00
Published on Web 07/24/2007

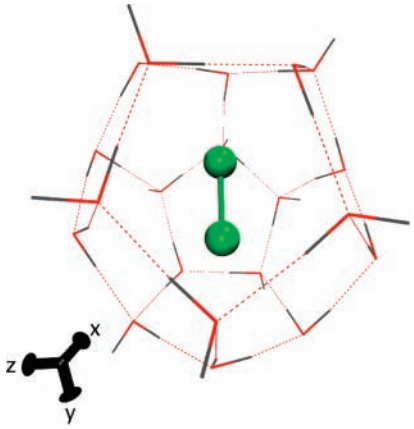

Figure 1. The RIMP2/A′ VDZ optimized structure of $Cl_2(H_2O)_{20}$.

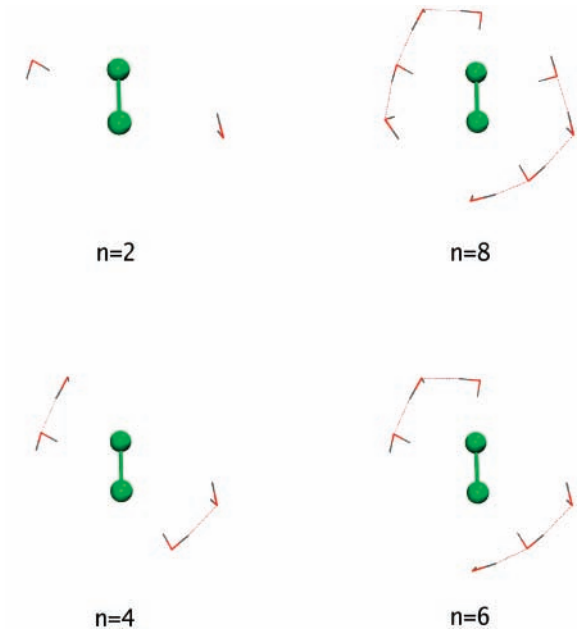

Figure 2. $Cl_2(H_2O)_n$, $n = 2$, 4, 6, and 8, clusters cut out of the $Cl_2(H_2O)_{20}$ model of chlorine hydrate.

of the cage, and the geometry of the $Cl_2(H_2O)_{20}$ system was optimized, retaining inversion symmetry, with the RIMP2[20,21] method and a A′ VDZ basis set consisting of the aug-cc-pVDZ basis set[16] on the chlorine atoms and the cc-pVDZ basis set[22] on the oxygen and hydrogen atoms. The optimized geometry of $Cl_2(H_2O)_{20}$, shown in Figure 1, was then employed in RICC2 calculations of the energies and the oscillator strengths of the transitions from the 1^1 A_g ground state to the seven lowest lying excited states in both the A_g and A_u symmetry blocks of the singlet and triplet manifolds. These calculations were carried out by using the A′ VDZ basis set as well as the full aug-cc-pVDZ basis set.[23] Nearly the same excitation energies were obtained with the two basis sets, and only the smaller A′ VDZ basis set was used in the RICC2 calculations of the excitation energies of $Cl_2(H_2O)_{24}$ and $Cl_2(H_2O)_n$, $n \leq 8$ subclusters (shown in Figure 2) cut out from the $Cl_2(H_2O)_{20}$ cluster.

RICC2/A′ VDZ calculations were also carried out on the $Cl_2(H_2O)_{24}$ cluster. In this case, the geometry of the $(H_2O)_{24}$ cage was taken from a proton disordered methane hydrate structure, with the positions of the oxygen atoms determined from the X-ray diffraction structure of ethylene oxide hydrate,[24] and the positions of the hydrogen atoms randomized according to the Bernal−Fowler rules.[25] The experimental gas-phase bond

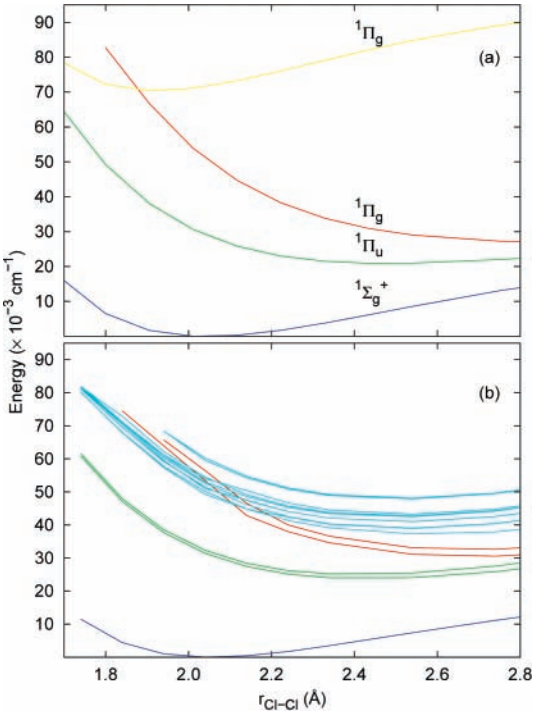

Figure 3. Potential energy curves of the low-lying singlet states of (a) Cl_2 and (b) $Cl_2(H_2O)_{20}$ calculated with the CC2/AVDZ and RICC2/A′ VDZ methods, respectively.

length[15] was employed for the Cl_2 molecule, which was located at the center of the cage, oriented along the long axis.

The CC2 and CC3 calculations were performed with the DALTON program,[26] and the RIMP2 and RICC2 calculations were performed with the Turbomole program.[27] The frozen core approximation was used in all calculations.

Results and Discussion

Cl_2. Table 1 reports for Cl_2 the vertical electronic excitation energies calculated with the CC2 and CC3 methods and use of the aug-cc-pVDZ, aug-cc-pVTZ, and aug-cc-pVTZ(+) basis sets. Table 1 also reports the excitation energies from the multireference CI (MRCISD) calculations of Peyerimhoff and Buenker,[28] and, where available, from experiment.[29−31]

The dominant electronic configuration of the $^1\Sigma_g^+$ ground state of Cl_2 is $\sigma_g^2\pi_u^4\pi_g^4\sigma_u^0$, where only the valence orbitals formed from overlap of the chlorine 3p orbitals are indicated. The low-lying valence transitions are dominated by single-electron excitations from the filled σ_g, π_u, and π_g orbitals into the unoccupied σ_u orbital. A number of doubly excited valence states exist, but, at the equilibrium geometry, these lie higher in energy than the lowest lying $\pi_g \rightarrow$ 4s Rydberg state, the vertical excitation energy of which is near 64 000 cm^{-1}.

At the CC2 level of theory, the excitation energies of the valence states of Cl_2 change by at most 530 cm^{-1} in going from the aug-cc-pVDZ to the aug-cc-pVTZ basis set, whereas the changes in the valence excitation energies in going from the aug-cc-pVTZ to the aug-cc-pVTZ(+) basis set are less than 5 cm^{-1}. As expected, the energies of the $\pi_g \rightarrow$ 4s Rydberg states drop appreciably upon inclusion of the Rydberg functions in the basis set. The vertical excitation energies calculated with the CC2 and CC3 methods are in fairly good agreement with each other, with the previously published MRCISD results,[28] and with experiment.[29−31] For the five valence states considered, the largest difference between the CC2 and CC3 calculated excitation energies is 2902 cm^{-1}, in the case of the $^1\Pi_g$ state.

TABLE 1: Vertical Excitation Energies (cm^{-1}) of Cl_2[a]

		CC2			CC3		
state	excitation	AVDZ	AVTZ	AVTZ(+)	AVTZ(+)	MRCISD[28]	exptl
$1^1\Pi_u$	$\pi_g \rightarrow \sigma_u$	31 814	31 922	31 921	31 214	32 504	30 726[29]
$1^1\Pi_g$	$\pi_u \rightarrow \sigma_u$	56 184	56 509	56 505	53 603	55 192	
$1^3\Pi_u$	$\pi_g \rightarrow \sigma_u$	25 163	25 728	25 730	25 448	26 132	26 841[b]
$1^3\Pi_g$	$\pi_u \rightarrow \sigma_u$	50 141	50 347	50 345	48 974	50 248	
$1^3\Sigma_u^+$	$\sigma_g \rightarrow \sigma_u$	55 802	55 718	55 715	54 663	54 846	
$2^3\Pi_g$	$\pi_g \rightarrow 4s$	69 214	68 205	63 181	63 520	67 267	63 800[31]
$2^1\Pi_g$	$\pi_g \rightarrow 4s$	70 633	69 338	63 826	64 229	67 589	64 100[31]

[a] All CC2 and CC3 calculations were performed at the experimental bond length of 1.9881 Å.[15] [b] Determined by using the ω_e, $\omega_e x_e$, and T_e values of ref 30.

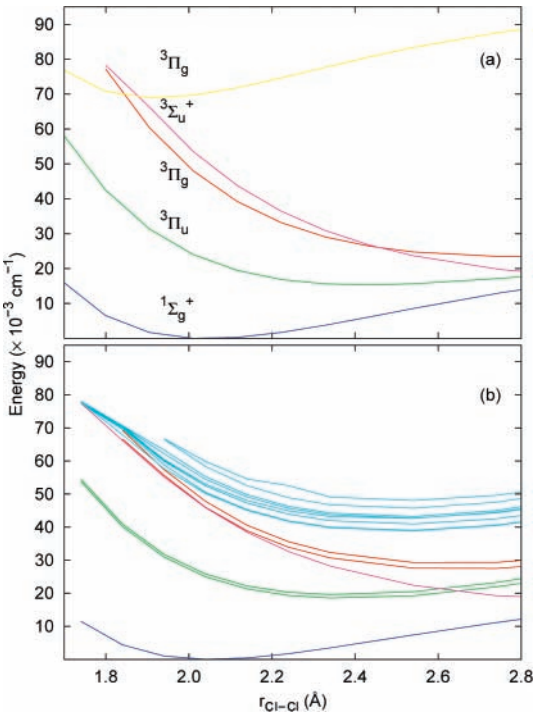

Figure 4. Potential energy curves of the low-lying triplet states of (a) Cl_2 and (b) $Cl_2(H_2O)_{20}$ calculated with the CC2/AVDZ and RICC2/A′ VDZ methods, respectively. The ground state singlet potential has been included for reference.

The CC2 and CC3 calculations with the aug-cc-pVTZ(+) basis set give excitation energies for the lowest singlet and triplet Rydberg states within 360 cm^{-1} of the experimental values. Within the electric dipole approximation the only allowed transition listed in Table 1 is that to the $1^1\Pi_u$ state, with an oscillator strength of 0.001 at the CC2/AVDZ level of theory.

Figures 3a and 4a depict potential energy curves for the ground state and low-lying excited states of Cl_2. The potential energy curve of the ground state was calculated at the CC2/AVDZ level and the excited-state potential energy curves were generated by adding the CC2 energy of the ground state to the CC2 excitation energies. As the CC2 method is based on a single reference configuration, the potential energy curves are expected to degrade for bond lengths appreciably greater than the equilibrium bond length (R_e) of the ground state.[14] For bond lengths up to about 1.2 times R_e, the CC2 potential energy curves for the valence states of Cl_2 are in good agreement with the corresponding MRCISD potential energy curves.[28,32,33]

$Cl_2(H_2O)_{20}$. For the optimized structure of $Cl_2(H_2O)_{20}$ shown in Figure 1, the chlorine molecule is essentially aligned between two opposing oxygen atoms. The calculated Cl_2 bond length is 2.04 Å, nearly the same as that calculated for the isolated Cl_2 molecule. If the Cl_2 molecule is rotated from its orientation in the optimized structure to along the *x*-, *y*-, or *z*-axis of the molecular frame, the energy increases by 5.0 to 12.5 kcal/mol.

TABLE 2: Calculated Vertical Excitation Energies and Oscillator Strengths of $Cl_2(H_2O)_{20}$

	RICC2/A′ VDZ			
excited state symmetry	ΔE (cm^{-1})	f	RICC2/AVDZ ΔE (cm^{-1})	assignment[a]
$1\ ^1A_u$	31 415	0.001	31261	$^1\Pi_u$
$2\ ^1A_u$	32 344	0.0006	32209	$^1\Pi_u$
$1\ ^1A_g$	49 270	0	49269	CT
$3\ ^1A_u$	50 129	0.1	50149	CT
$2\ ^1A_g$	51 023	0	51042	CT
$4\ ^1A_u$	51 500	0.3	51546	CT
$5\ ^1A_u$	52 638	0.01	52843	CT
$3\ ^1A_g$	52 965	0	53101	CT
$4\ ^1A_g$	53 417	0	53293	$^1\Pi_g$ + CT
$5\ ^1A_g$	53 984	0	53981	CT
$1\ ^3A_u$	24 978	0	24902	$^3\Pi_u$
$2\ ^3A_u$	25 841	0	25789	$^3\Pi_u$
$3\ ^3A_u$	45 850	0	45991	$^3\Sigma_u^+$ + CT
$1\ ^3A_g$	45 999	0	45860	$^3\Pi_g$ + CT
$2\ ^3A_g$	47 779	0	47606	$^3\Pi_g$ + CT
$4\ ^3A_u$	50 200	0	50273	CT
$3\ ^3A_g$	50 525	0	50567	CT
$4\ ^3A_g$	52 454	0	52645	CT
$5\ ^3A_u$	52 483	0	52689	CT
$5\ ^3A_g$	53 023	0	53095	CT

[a] States with the excitation localized on the Cl_2 molecule are labeled as they would be for isolated Cl_2.

Counterpoise corrected[34] RIMP2 calculations predict that the $Cl_2(H_2O)_{20}$ cluster is 2.3 kcal/mol more stable than the empty $(H_2O)_{20}$ cage and a free Cl_2 molecule, when retaining the cluster optimized geometries for the fragments. For comparison, we note that similar calculations predict a 3.4 kcal/mol interaction between the CH_4 molecule and the $(H_2O)_{20}$ cage in a CH_4-$(H_2O)_{20}$ cluster model of an occupied 5^{12} cage of methane hydrate.[35]

Table 2 lists the calculated electronic transition energies and oscillator strengths for $Cl_2(H_2O)_{20}$. The five lowest energy excited states in both the A_g and A_u symmetry blocks and in both the singlet and triplet manifolds are reported. The calculated potential energy curves along the Cl−Cl stretching coordinate are shown in Figures 3b and 4b. Inclusion of diffuse basis functions on the water molecules is found to have little effect on the excitation energies for the considered states of $Cl_2(H_2O)_{20}$, with the changes being at most 200 cm^{-1}. On the other hand, the calculated vertical transition energies change by up to 700 cm^{-1} upon expansion of the basis set on the chlorine atoms from aug-cc-pVDZ to aug-cc-pVTZ. These changes are comparable to those found for the isolated Cl_2 molecule with the same basis set change. In light of these results, it is concluded

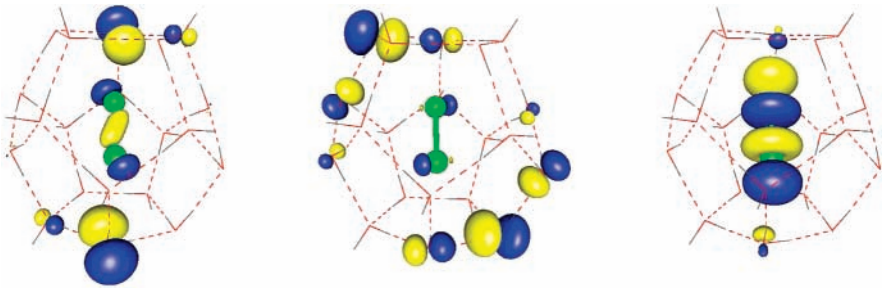

Figure 5. The $54a_g$, $56a_g$, and $59a_u$ molecular orbitals of $Cl_2(H_2O)_{20}$.

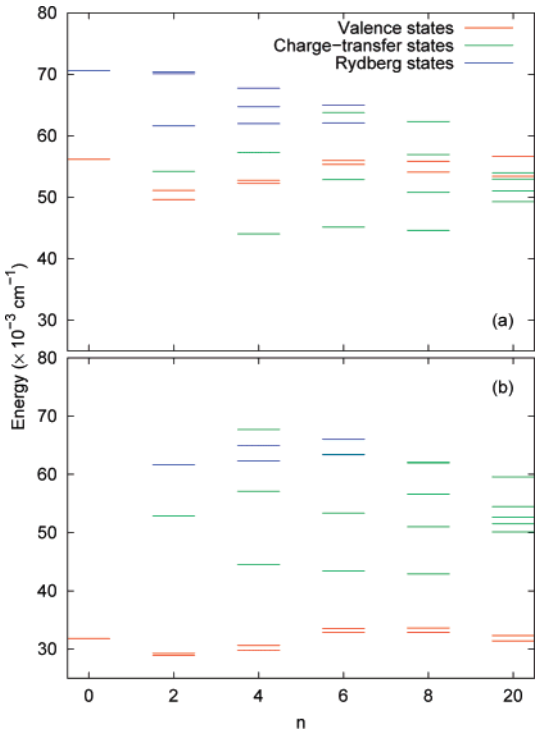

Figure 6. Singlet excitation energies of Cl_2 and the $Cl_2(H_2O)_n$ cluster models calculated with the CC2/AVDZ and RICC2/A′ VDZ methods, respectively: (a) A_g states and (b) A_u states. Valence, charge-transfer, and Rydberg states are denoted by red, green, and blue, respectively.

that the A′ VDZ basis set is adequate for providing a qualitative picture of the differences in the low-lying excited states of Cl_2, $Cl_2(H_2O)_{20}$, and $Cl_2(H_2O)_{24}$.

The low-lying $^1\Sigma_g^+ \rightarrow 1^3\Pi_u, ^1\Sigma_g^+ \rightarrow 1^1\Pi_u$ valence type transitions of Cl_2 are calculated to shift by at most 720 cm^{-1} in going from the isolated molecule to the $Cl_2(H_2O)_{20}$ complex. Due to the loss of symmetry, the Π_u states are split into A_g and A_u states, with the splittings being about 1000 cm^{-1}. Although only three states ($1^3\Pi_g$, $1^3\Sigma_u^+$, and $^1\Pi_g$) of Cl_2 exist in the 45 000−57 000 region, 20 states are predicted in this energy region for $Cl_2(H_2O)_{20}$. The plethora of new states in the complex is the result of water-to-Cl_2 charge-transfer transitions. These are dominated by configurations in which an electron is transferred from the lone-pair orbits of the water molecules to the LUMO ($59a_u$) of the Cl_2 molecule. The valence $1^3\Pi_g$, $1^3\Sigma_u^+$, and $1^1\Pi_g$ states expected in this energy range are mixed with the charge transfer states. Of the four $^1A_g \rightarrow {}^1A_u$ charge-transfer transitions calculated for $Cl_2(H_2O)_{20}$, two have large oscillator strengths. The lower energy of these (at 51 500 cm^{-1}) is dominated by the $54a_g \rightarrow 59a_u$ transition, and the higher energy of these, at 52 638 cm^{-1}, is essentially $56a_g \rightarrow 59a_u$ in character. The $54a_g$, $56a_g$, and $59a_u$ orbitals are depicted in Figure 5.

As seen from Figures 3b and 4b all the charge transfer states of $Cl_2(H_2O)_{20}$ are repulsive near the equilibrium geometry of the cluster, although several of the states have shallow minima near $R_{Cl-Cl} = 2.5$ Å, about 0.4 Å greater than that of the equilibrium structure. These states could decay by a nonadiabatic transition to a lower lying valence state of the cluster. Alternatively, the hole on the water cage could lead to dissociation of a water molecule, and subsequent rearrangement to an Eigen or Zundel ion. The experiments on bromine hydrate provide evidence of fast (∼50 fs) dynamics of the charge transfer state,[36] but the nature of the rearrangement responsible for the fast decay is not known.

The excitation energies calculated for $Cl_2(H_2O)_{24}$ are close to those for $Cl_2(H_2O)_{20}$, with the energies of the low-lying valence states of the two clusters agreeing within 500 cm^{-1}. However, the charge transfer states fall 1700−3000 cm^{-1} lower in energy in the larger cluster as a result of the destabilization of some of the high-lying water lone-pair orbitals in going from the $Cl_2(H_2O)_{20}$ to the $Cl_2(H_2O)_{24}$ cluster.

$Cl_2(H_2O)_n$. It is instructive to follow the evolution of the electronic states of the $Cl_2(H_2O)_n$ clusters with increasing n. These results are summarized in Figure 6. Interestingly, the $Cl_2(H_2O)_2$ cluster has low-lying (∼53 000 cm^{-1}) water-to-Cl_2 charge transfer states of A_g and A_u symmetry. As n increases from 2 to 8, the number of low-lying charge transfer states grows, with the lowest charge transfer states dropping in energy from ∼53 000 cm^{-1} in the $n = 2$ cluster to ∼45 000 cm^{-1} in the $n = 4$, 6, and 8 clusters, before climbing back up to ∼50 000 cm^{-1} in the $n = 20$ cluster. The $n = 2-6$ clusters also possess Rydberg states in the 62 000−70 000 cm^{-1} range. These include the Cl_2 $\pi_g \rightarrow 4s$ Rydberg transition as well as transitions that can be characterized as water lone-pair to Cl_2 4s. Presumably these transitions would also be found for the $n = 8$, 20, and 24 systems if a sufficient number of excited states were extracted.

Conclusions

The RICC2 method has been used to calculate the electronic absorption spectra of Cl_2, $Cl_2(H_2O)_{20}$, and $Cl_2(H_2O)_{24}$. For all three species the low-lying transitions near 30 000 cm^{-1} are due to the Cl_2 $\pi_g \rightarrow \sigma_u$ transition. In Cl_2, the next group of transitions is also valence-like and occurs near 50 000 cm^{-1}. In contrast, in $Cl_2(H_2O)_{20}$ and $Cl_2(H_2O)_{24}$ there is a dense manifold of charge transfer states starting near 45 000 cm^{-1}. The charge transfer states involve excitation of an electron from the lone-pair orbitals of the $(H_2O)_{20}$ and $(H_2O)_{24}$ cages to the σ_u-like orbital of the chlorine, and carry oscillator strengths up to 300 times greater than the most intense valence transitions of the isolated Cl_2 molecule. These results are consistent with the recently measured absorption spectrum of bromine hydrate, where there are intense transitions beginning near 41 700 cm^{-1} which have been assigned to a charge-transfer process.

Acknowledgment. We acknowledge support from the National Science Foundation through grant CHE-0404743.

D.P.S. wishes to acknowledge the New Zealand Foundation for Research, Science and Technology for a Postdoctoral Fellowship. We also acknowledge valuable discussions with Profs. Ken Janda and Ara Apkarian.

References and Notes

(1) Sloan, E. D., Jr. *Nature* **2003**, *426*, 353−359.
(2) Buffett, B. A. *Annu. Rev. Earth Planet. Sci*. **2000**, *28*, 477−507.
(3) Davy, H. *Philos. Trans. R. Soc. London* **1811**, *101*, 155−162.
(4) Pauling, L.; Marsh, R. E. *Proc. Natl. Acad. Sci*. U.S.A. **1952**, *38*, 112−118.
(5) Kerenskaya, G.; Goldschleger, I. U.; Apkarian, V. A.; Janda, K. C. *J. Phys. Chem. A* **2006**, *110*, 13792−13798.
(6) Patchkovskii, S.; Yurchenko, S. N. *Phys. Chem. Chem. Phys*. **2004**, *6*, 4152−4155.
(7) Claussen, W. F. *J. Chem. Phys.* **1951**, *19*, 1425−1426.
(8) Cady, G. H. *J. Phys. Chem.* **1981**, *85*, 3225−3230.
(9) Hattig, C.; Weigend, F. *J. Chem. Phys.* **2000**, *113*, 5154−5161.
(10) Hattig, C.; Hald, K. *Phys. Chem. Chem. Phys.* **2002**, *4*, 2111−2118.
(11) Hattig, C.; Kohn, A. *J. Chem. Phys.* **2002**, *117*, 6939−6951.
(12) Christiansen, O.; Koch, H.; Jørgensen, P. *Chem. Phys. Lett*. **1995**, *243*, 409−418.
(13) Christiansen, O.; Koch, H.; Jørgensen, P. *J. Chem. Phys.* **1995**, *103*, 7429−7441.
(14) Koch, H.; Christiansen, O.; Jørgensen, P.; de Meras, A. M. S.; Helgaker, T. *J. Chem. Phys.* **1997**, *106*, 1808−1818.
(15) Clyne, M. A. A.; Coxon, J. A. *J. Mol. Spectrosc*. **1970**, *33*, 381−406.
(16) Woon, D. E.; Dunning, T. H., Jr. *J. Chem. Phys.* **1993**, *98*, 1358−1371.
(17) Dunning, T. H., Jr.; Harrison, P. J. *Modern Theoretical Chemistry*; Plenum Press: New York, 1977; Vol. 2.
(18) McDonald, S.; Ojamae, L.; Singer, S. *J. Phys. Chem. A* **1998**, *102*, 2824−2832.
(19) Kuo, J.-L.; Coe, J. V.; Singer, S. J.; Band, Y. B.; Ojamae, L. *J. Chem. Phys.* **2001**, *114*, 2527−2540.
(20) Weigend, F.; Häser, M. *Theor. Chem. Acc.* **1997**, *97*, 331−340.
(21) Weigend, F.; Häser, M.; Patzelt, H.; Ahlrichs, R. *Chem. Phys. Lett*. **1998**, *294*, 143−152.
(22) Dunning, T. H., Jr. *J. Chem. Phys.* **1989**, *90*, 1007−1023.
(23) Kendall, R. A.; Dunning, T. H., Jr.; Harrison, R. J. *J. Chem. Phys.* **1992**, *96*, 6796−6806.
(24) McMullan, R. K.; Jeffrey, G. A. *J. Chem. Phys.* **1965**, *42*, 2725−2732.
(25) Bernal, J. D.; Fowler, R. H. *J. Chem. Phys.* **1933**, *1*, 515−548.
(26) Dalton, a molecular electronic structure program, release 2.0 (2005) see: http://www.kjemi.uio.no/software/dalton/dalton.html.
(27) Ahlrichs, R.; Bär, M.; Häser, M.; Horn, H.; Kölmel, C. *Chem. Phys. Lett*. **1989**, *162*, 165−169.
(28) Peyerimhoff, S. D.; Buenker, R. J. *Chem. Phys.* **1981**, *57*, 279−296.
(29) Coxon, J. A. *Molecular Spectroscopy*; Chemical Society, 1973; Vol. 1.
(30) Ishiwata, T.; Ishiguro, A.; Obi, K.; Tanaka, I. *Chem. Phys. Lett*. **1989**, *159*, 594−598.
(31) Jureta, J.; Cvejanović, S.; Kurepa, M.; Cvejanović, D. *Z. Phys. A* **1982**, *304*, 143−153.
(32) Kokh, D. B.; Alekseyev, A. B.; Buenker, R. J. *J. Chem. Phys.* **2004**, *120*, 11549−11556.
(33) Kokh, D. B.; Alekseyev, A. B.; Buenker, R. J. *J. Chem. Phys.* **2001**, *115*, 9298−9310.
(34) Boys, S.; Bernardi, F. *Mol. Phys.* **1970**, *19*, 553−566.
(35) McCarthy, V. N.; Jordan, K. D. *Chem. Phys. Lett*. **2006**, *429*, 166−168.
(36) Apkarian, V. A.; Janda, K. C. Private communication.